

thank the Daresbury Laboratory for use of facilities and provision of beam time. We also thank the NATO Scientific Affairs Bureau for the award of a travel grant (RG.82/0139) to N.J.B. and K.D.K.

Registry No. 1, 114301-10-9; 2, 114301-13-2; 3, 112022-71-6; 3', 114301-11-0; 4, 98218-48-5; 5, 114301-14-3; 6, 112022-74-9; 7, 82384-

51-8; 8, 88920-97-2; 9, 86593-50-2; N3PY2, 88917-40-2; N3ORPY2, 114301-08-5; N4PY2, 98218-51-0.

Supplementary Material Available: Tables 5-12 of raw (background-subtracted) EXAFS data for compounds 2, 3', 7, 8, 9, 6, 4, and 5 respectively (70 pages). Ordering information is given on any current masthead page.

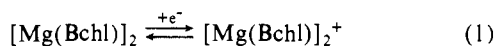
Metal Complexes with Tetrapyrrole Ligands. 50.¹ Redox Potentials of Sandwichlike Metal Bis(octaethylporphyrinates) and Their Correlation with Ring-Ring Distances

Johann W. Buchler* and Bernd Scharbert

Contribution from the Institut für Anorganische Chemie, Technische Hochschule Darmstadt, D-6100 Darmstadt, Germany. Received October 13, 1987

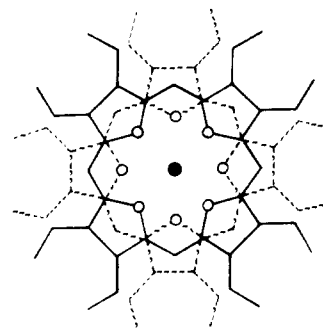
Abstract: On the basis of prior work describing the synthesis and structure of sandwichlike metal bis(porphyrinates) $M(\text{OEP})_2$ (1; $M = \text{Y, La, ... , Lu}$, except Pm), the electron-transfer reactions of these double-deckers are presented. Apart from the Ce^{IV} complex $\text{Ce}(\text{OEP})_2$ (1c), all the other species contain M^{III} ions that are not affected in the redox reactions. The neutral M^{III} complexes 1 are porphyrin π -radicals yielding the porphyrin π -diradical cations $[M(\text{OEP})_2]^+$ (2) upon reversible one-electron oxidation and the monoanions $[M(\text{OEP})_2]^-$ (3) or the porphyrin π -radical dianions $[M(\text{OEP})_2]^{2-}$ (4) upon reversible one- or two-electron reduction. $\text{Ce}(\text{OEP})_2$ (1c) is reversibly oxidized to the porphyrin π -radical cation $[\text{Ce}(\text{OEP})_2]^+$ (2c). The quasi-reversible reduction of 1c gives the anion $[\text{Ce}(\text{OEP})_2]^-$ (3c) with Ce^{III} . For the neutral M^{III} complexes 1, the energies of the near-infrared absorption bands and the redox potentials for the processes $1 \rightleftharpoons 2$ are correlated with the ionic radii r_1 of the trivalent central ions M^{III} . A decrease of the ring oxidation potentials parallels a decrease of the ionic radii and, hence, the ring-ring distances in the double-deckers.

A bacteriochlorophyll *b* dimer $[\text{Mg}(\text{Bchl})]_2$,² the "special pair", represents the reaction center of bacterial photosynthesis. It is embedded in an extended membrane protein complex and, according to present knowledge, is oxidized by absorption of light quanta according eq 1, which causes the primary charge separation.³



In the special pair, two tetrapyrrole ligands interact via a π - π overlap between two pyrrole rings, one of each macrocycle,⁴ at a distance of about 300 pm.³

Recently, we prepared the sandwichlike metal octaethylporphyrinates $M(\text{OEP})_2$ (1a-p; see Table I)⁵⁻¹⁰ including yttrium,



● = M (metal); ○ = N (nitrogen)

$[M(\text{OEP})_2]^{n-}$: 1, $n = 0$; 2, $n = 1+$; 3, $n = 1-$; 4, $n = 2-$. For specification of metals, see Table I.

lanthanum, and all metals of the lanthanoid series except promethium, following our previous work on the similar tetra-*p*-tolylporphyrin double-deckers $M(\text{TTP})_2$ ($M = \text{Ce, Pr, Nd}$).^{11,12} Suslick and co-workers recently obtained the actinide derivatives $\text{Th}(\text{TPP})_2$ and $\text{U}(\text{TPP})_2$.¹³

The idea has been expressed that these double-deckers show analogies to the special pair in regard to structure and electron configuration.^{8,12,14} The structural analogy lies in the face-to-face arrangement of two tetrapyrrole macrocycles. This causes the electronic analogy seen in the following observations: (1) The abstraction of an electron from the porphyrin π -orbitals is easier

(1) Paper 49. Botulinski, A.; Buchler, J. W.; Lee, Y. J.; Scheidt, W. R.; Wicholas, M. *Inorg. Chem.* **1988**, *27*, 927-933.

(2) Abbreviations used: Bchl, bacteriochlorophyll *b*; M, metal; (P)²⁻, (OEP)²⁻, (Pc)²⁻, (TPP)²⁻, (TTP)²⁻, (TCIP)²⁻, and (TAP)²⁻ are dianions of a general porphyrin, 2,3,7,8,12,13,17,18-octaethylporphyrin, phthalocyanine, 5,10,15,20-tetraphenylporphyrin, 5,10,15,20-tetra-*p*-tolylporphyrin, 5,10,15,20-tetrakis(*p*-chlorophenyl)porphyrin, and 5,10,15,20-tetra-*p*-anisylporphyrin, respectively; Ln, lanthanoid metal; DMF, dimethylformamide; H(acac), acetylacetonate; near-IR, near-infrared; SCE, saturated calomel electrode; THF, tetrahydrofuran.

(3) (a) Deisenhofer, J.; Epp, O.; Miki, K.; Huber, R.; Michel, H. *Nature (London)* **1985**, *318*, 618-624. (b) Deisenhofer, J.; Epp, O.; Miki, K.; Huber, R.; Michel, H. *J. Mol. Biol.* **1984**, *180*, 385-398.

(4) Plato, M.; Tränkle, E.; Lubitz, W.; Lenzian, F.; Möbius, K. *Chem. Phys.* **1986**, *107*, 185-196, and references cited therein.

(5) Buchler, J. W.; De Cian, A.; Fischer, J.; Kihn-Botulinski, M.; Paulus, H.; Weiss, R. *J. Am. Chem. Soc.* **1986**, *108*, 3652-3659.

(6) Buchler, J. W.; De Cian, A.; Fischer, J.; Kihn-Botulinski, M.; Weiss, R. *Inorg. Chem.* **1988**, *27*, 339-345.

(7) Buchler, J. W.; Knoff, M. In *Optical Properties and Structure of Tetrapyrroles*; Blauer, G.; Sund, H., Eds.; de Gruyter: Berlin, 1985; pp 91-105.

(8) (a) Buchler, J. W.; Elsässer, K.; Kihn-Botulinski, M.; Scharbert, B. *Angew. Chem.* **1986**, *98*, 257-258; *Angew. Chem., Int. Ed. Engl.* **1986**, *25*, 286-287. (b) Scharbert, B. Doctoral Dissertation, Technische Hochschule Darmstadt, 1988.

(9) Buchler, J. W.; Hüttermann, J.; Löffler, J. *Bull. Chem. Soc. Jpn.* **1988**, *61*, 71-77.

(10) (a) Buchler, J. W.; Kihn-Botulinski, M., to be submitted for publication. (b) Kihn-Botulinski, M. Doctoral Dissertation, Technische Hochschule Darmstadt, 1986.

(11) Buchler, J. W.; Kapellmann, H. G.; Knoff, M.; Lay, K. L.; Pfeifer, S. Z. *Naturforsch., B: Anorg. Chem., Org. Chem.* **1983**, *38B*, 1339-1345.

(12) Buchler, J. W.; Elsässer, K.; Kihn-Botulinski, M.; Scharbert, B.; Tansil, S. *ACS Symp. Ser.* **1986**, *321*, 94-104.

(13) Girolami, G. S.; Milam, S. N.; Suslick, K. N. *Inorg. Chem.* **1987**, *26*, 343-344.

(14) Buchler, J. W. *Comments Inorg. Chem.* **1987**, *6*, 175-191.

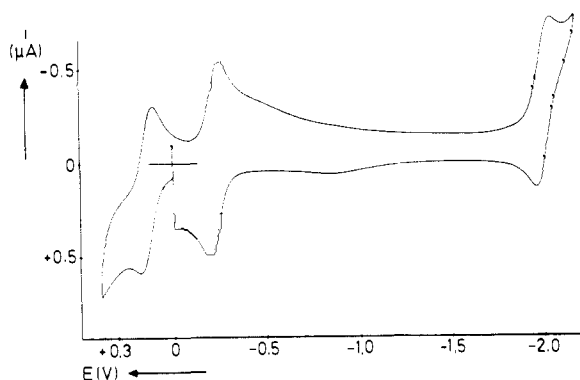


Figure 1. Cyclic voltammogram of $\text{Er}(\text{OEP})_2$ (**1l**) in TBAH/DMF; concentration 1.6×10^{-4} mol/L, voltage scan rate 0.1 V/s.

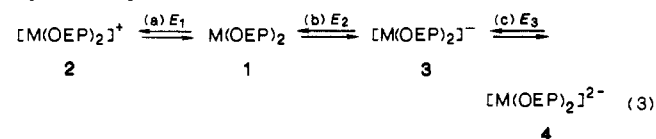
A Beckman Pt-button electrode was used as the working electrode, the electroactive surface A of which was determined by cyclic voltammetry²² [$A = 2.24i_p/nFc_0[(nF/RT)vD]^{1/2}$] and checked by chronoamperometry²³ [$A = \pi^{1/2}i_p^{1/2}/nFc_0D^{1/2}$] of the $[\text{Fe}(\text{CN})_6]^{4-/3-}$ pair ($\text{K}_4[\text{Fe}(\text{CN})_6]$ in 0.1 M aqueous KCl) for which D is known.²⁴ Thus, in turn, with known A , D was determined for all **1** except **1c** from the peak currents of the reversible reduction waves E_2 and checked for **1d** by chronoamperometry. A value of $D = (2.4 \pm 0.2) \times 10^{-6}$ cm² s⁻¹ was found for all **1** except **1c** for which the first reduction process is quasi-reversible. However, because all molecules **1** have practically identical shapes, $D = 2.4 \times 10^{-6}$ cm² s⁻¹ is safely assumed for **1c** as well.

(d) Electron-Transfer Rate for the Reduction of $\text{Ce}(\text{OEP})_2$ (1c**).** The quasi-reversible nature²⁵ of the reduction of **1c** was demonstrated by studying the dependence of the difference ΔE_p on c_0 and v , which were varied in the ranges of $(0.40\text{--}4.20) \times 10^{-4}$ mol/L and 2–200 mV/s, respectively. ΔE_p increased monotonously with v but remained essentially independent of c_0 in this variation. When the procedure of Nicholson²⁶ was used, the electron-transfer rate k_s was determined^{8b} with the assumption that D is equal for **1c** and its reduction product **3c** and that the transfer coefficient α equals 0.5. Thus, from three measurements, a value of $k_s = (2.2 \pm 1.0) \times 10^{-3}$ cm s⁻¹ was obtained. This value was checked with a new computer-assisted fitting procedure developed by Speiser,^{25,27} which allows the simultaneous extraction of α and k_s from the cyclic voltammetry data using ΔE_p , $E_p - E_0$, and the normalized current function $\pi^{1/2}\chi(nFvt/RT)$.²² For this procedure, the range of measured voltage scan rates was extended to 8 V s⁻¹. The values for individual measurements obtained by this method matched the ones obtained according to Nicholson and Shain within $\pm 2\%$. Thus, the assumption $\alpha = 0.5$ was justified.

(e) Spectroelectrochemistry of $\text{PrH}(\text{OEP})_2$ (1b**).** A total of 25 mg (0.021 mmol) **1b** was electrolyzed in 75 mL of a 0.1 M $\text{LiClO}_4/\text{DMF}$ solution at +0.30 V with simultaneous sonification of the electrolysis cell. The working electrode was a cylindrical Pt net ($r = 17.5$ mm, $h = 50$ mm). Within 45 min, the current dropped from 4 to 0.5 mA when 3.6 C (1.8 faradays/mol) had been transported. At 2.4 and 3.55 C, samples were withdrawn from the cell and UV/vis and near-IR spectra taken (see Figure 2).

Results and Discussion

(a) Cyclic Voltammetry. The redox behavior of the complexes **1** was determined by cyclic voltammetry. A typical voltammogram is shown in Figure 1. Generally, three reversible one-electron processes (eq 3, a–c) are found for the $\text{M}(\text{OEP})_2$ with trivalent central metals. The individual half-wave potentials E_1 , E_2 , and E_3 are compiled in Table II.



(b) Identification of the Ions 2–4. The one-electron oxidation product **2c** for $\text{M} = \text{Ce}$ has been identified before as a π -radical

Table II. Redox Potentials of the Complexes $\text{M}(\text{OEP})_2$ (**1a–p**) in 0.2 M $\text{NBu}_4\text{PF}_6/\text{DMF}$ vs SCE^a in Correlation with the Ionic Radii^b r_1 of M^{3+} (E_1 , E_2 , and E_3 Correspond to Equations 3a–c, Respectively)

	M	r_1 , pm	E_1 , V	E_2 , V	E_3 , V
1a	Y	101.5	0.14	-0.21	c
1b	La	118	c	-0.01	-1.935
1c	Ce	97 ^d	0.33	-0.47 ^e	-1.935 ^f
1d	Pr	114	0.24	-0.08	-1.96
1e	Nd	112	0.225	-0.095	-1.96
1f	Sm	109	0.205	-0.13	-1.965
1g	Eu	107	0.185	-0.15	-1.97
1h	Gd	106	0.18	-0.165	-1.97
1i	Tb	104	0.17	-0.18	-1.98
1j	Dy	103	0.155	-0.20	-1.985
1k	Ho	102	0.15	-0.215	-1.985
1l	Er	100	0.135	-0.225	-1.995
1m	Tm	99	0.12	-0.235	-1.995
1n	Yb	98	0.115	-0.25	-1.995
1p	Lu	97	0.10	-0.265	-2.00

^aThe uncertainty in each potential is ± 5 mV. ^bFor coordination number 8.¹⁵ ^cNot observed because of beginning decomposition of the supporting electrolyte. ^dFor Ce^{IV} ; $r_1 = 114$ pm¹⁵ for Ce^{III} . ^eQuasi-reversible electron transfer. ^fThis process involves a Ce^{III} species.

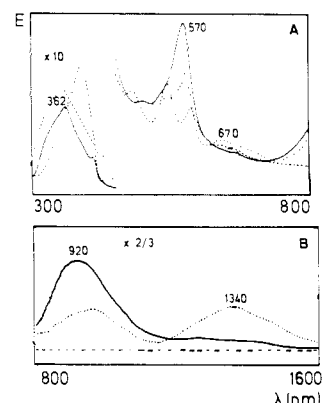


Figure 2. UV/vis (A) and near-IR spectrum (B) of electrogenerated $[\text{Pr}(\text{OEP})_2]\text{ClO}_4$ (—, taken at 1.8 e/molecule), the intermediate $\text{Pr}(\text{OEP})_2$ (---, taken at 1.2 e/molecule), and the educt $\text{PrH}(\text{OEP})_2$ (---) in DMF (see the Experimental Section).

cation.^{8a} For all the other trivalent central metals, these species are bis(π -radical) cations. This was exemplified by electrolysis of $\text{PrH}(\text{OEP})_2$, the conjugate acid of **3d**, which was obtained from $\text{Pr}(\text{OEP})_2$ (**1d**) by treatment with hydrazine hydrate. About 2 e/molecule served to produce the spectrum shown in Figure 2. This spectrum is very similar to the dimer $[\text{Zn}(\text{OEP})\text{Br}]_2$ of the porphyrin π -radical $\text{Zn}(\text{OEP})\text{Br}$, which is formed on cooling of the latter.²⁸ Obviously, the same kind of coupled bis(π -radical) is encountered already at room temperature in **2d**. The central metal serves as a clamp holding the two π -radicals together. Thus, for M^{III} , the species **2** can be regarded with confidence as bis(π -radical) cations.

The anions **3** are already described for $\text{M} = \text{Y}^9$ and Eu .⁶ They can be obtained by sodium anthracenide reduction of **1** in THF solution and have been characterized by ¹H NMR spectroscopy.^{6,8b,9,10b} They are easily hydrolyzed to the species $\text{MH}(\text{OEP})_2$. The NMR data and the absence of near-IR absorption confirm the absence of any π -radical character in **3**. The Y, La, and Lu derivatives **3a**, **3b**, and **3p**, respectively, are diamagnetic. Thus, on formation of **3**, reduction at the electron-deficient porphyrin ring occurs at all **1** containing M^{III} ions.

The reduction of the Ce^{IV} sandwich **1c** to **3c**, however, is a special case. This was not discussed but was already seen in the original cyclic voltammogram,^{8a} where the reduction at $E_2 = -0.47$ V is indeed "quasi-reversible". When the classical procedure of Nicholson²⁶ and a new method of Speiser^{25,27} are used, the elec-

(22) Nicholson, R. S.; Shain, I. S. *Anal. Chem.* **1964**, *36*, 706–723.

(23) Speiser, B. *Chem. in Unserer Zeit* **1981**, *15*, 21–26.

(24) Arvia, A. J.; Bazan, J. C.; Carozza, J. S. *W. Electrochim. Acta* **1968**, *13*, 81–90.

(25) Speiser, B. *Anal. Chem.* **1985**, *57*, 1390–1397.

(26) Nicholson, R. S. *Anal. Chem.* **1965**, *37*, 1351–1355.

(27) Speiser, B.; Scharbert, B., submitted for publication in *J. Chemom.*

(28) Fuhrhop, J. H.; Wasser, P.; Riesner, D.; Mauzerall, D. *J. Am. Chem. Soc.* **1972**, *94*, 7996–8001.

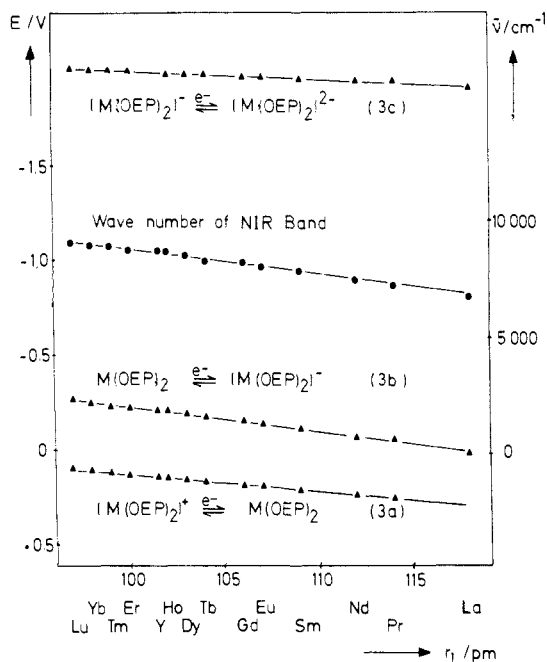


Figure 3. Redox potentials E (V; in 0.2 M $\text{NBu}_4\text{PF}_6/\text{DMF}$ vs SCE) and wavenumber $\bar{\nu}$ (cm^{-1}) of the near-IR absorption maxima of the sandwich complexes $\text{M}(\text{OEP})_2$ (1a–b,d–p) as functions of the ionic radii r_1 (pm; coordination number 8) of the trivalent central metal M.

tron-transfer rate constant k_s for this process was found to be $(2.2 \pm 1.0) \times 10^{-3} \text{ cm s}^{-1}$. Therefore, the electron exchange between 1c and the electrode is just retarded while the integrity of the redox components is retained. This retardation may be due to the fact that, contrary to all other 1, the central ion in 1c is reduced from Ce^{IV} to Ce^{III} . Because the central ion is hidden in the sandwich and the f orbital that has to lodge the incoming electron does not reach very far out, this metal redox reaction may be impeded as compared with the other ring redox reactions.

The involvement of the Ce^{IV} ion in the reduction was demonstrated in the tetraarylporphyrin series by isolation of the tetrakis(*p*-chlorophenyl)porphyrin derivative $\text{NBu}_4[\text{Ce}(\text{TCIP})_2]$ electrogenerated from $\text{Ce}(\text{TCIP})_2$ ($E_2 = -0.11 \text{ V}$ in dichloromethane).^{8b} The UV/vis spectrum²⁹ of this salt is very similar to the known spectrum of the well-defined Pr^{III} derivative $\text{NBu}_4[\text{Pr}(\text{TTP})_2]$.¹¹ If ring reduction had occurred—and this is not expected at a potential close to 0 V—it would have produced a porphyrin π -radical anion. Such anions are known to have strong visible absorption at 700 and 900 nm,³⁰ and this is absent in the sandwich anions $[\text{M}(\text{P})]^-$. The presence of Ce^{III} in 3c is furthermore indicated in the following observation: The potential E_3 for the step $3c \rightleftharpoons 4c$ nearly fits the correlation with the ionic radii shown in Figure 3 (see below). The ionic radii being equal for Ce^{III} and Pr^{III} , the corresponding redox potential E_3 for Ce^{III} is only slightly above the value for Pr^{III} (see Table II).

As the anions 3 all contain M^{III} ions, which are difficult to reduce, the further reduction of these is thought to yield porphyrin π -radical dianions $[\text{M}(\text{OEP})_2]^{2-}$ (4) with an extra electron in the π -cloud of one of the porphyrin rings. This view is suggested by the fact that E_3 is very low for all 4, (including 4c with Ce^{III}) and that there is only a small but steady variation with the ionic radius of the M^{III} ion (see Figure 3).

(c) Correlation of Redox Potentials, Ionic Radii, and Ring–Ring Distance. Not only the energies of the near-IR absorption bands but the redox potentials may be correlated with r_1 of the trivalent central metals (see Figure 3). The potentials E_1 and E_2 for $\text{Ce}(\text{OEP})_2$ (1c) cannot be accommodated with this graph, because Ce^{IV} complexes are involved, and, as just stated, only E_3 fits the line for 4c.

There is a rather narrow stability range for the neutral species 1 ($\pm 0.2 \text{ V}$; see Figure 2), which are either easily oxidized to 2 (eq 3a) or reduced to 3 (eq 3b). Thus, 1 shows typical properties of “mixed-valence” compounds.³¹ However, here, a mixed valence at the tetrapyrrole ligands, i.e. an “inverse mixed-valence complex”, is encountered in which two ligands in different oxidation levels are bridged by a common metal ion. The redox potentials E_1 and E_2 are such that 1 is the air-stable species.

The redox potentials E_1 to E_3 (see Figure 3) decrease with increasing r_1 in the same manner as the energies of the near-IR bands. Hence, they are determined by the ring–ring distance as well. An inductive effect of the central metal is excluded. On one hand, such an effect should be very small because of the small electronegativity differences within the lanthanoid series;³² on the other hand, it should produce the highest oxidation potentials with lutetium, the element with the largest electronegativity. There, however, the lowest values are observed. A “mesomeric” effect, i.e. the influence of the specific electron configuration of the lanthanoid ions, is not important either, because discontinuous changes of the data shown in Figure 1 should occur along the series of lanthanoid ions as is known with their optical spectra or magnetic susceptibilities. The importance of the size of the ions is also expressed by the observation that the data for $\text{Y}(\text{OEP})_2$,⁹ a group IIIA metal compound, nicely fit the correlation with the radii. Thus, the lanthanoid ion contraction can be detected not only optically but also electrochemically via the redox potentials (“electrochemical detection”).

A comparison of the slopes of the lines shown in Figure 3 is quite instructive. The redox potentials E_2 of the M^{III} complexes according to eq 3b, which formally correspond to the processes of eq 1 and 2 and produce the near-IR absorption upon oxidation, display with about $-92 \text{ cm}^{-1}/\text{pm}$ ³³ a large absolute value of the slope. This value is comparable to the value for the near-IR bands ($-99 \text{ cm}^{-1}/\text{pm}$). The energy level of this near-IR absorption therefore has some correspondence with the level of this redox potential.

Furthermore, the difference of the redox potentials E_2 and E_3 formally corresponds to the energy difference of a ligand oxidation ($3 \rightleftharpoons 1$) and a ligand reduction ($3 \rightleftharpoons 4$). As the first oxidation step involves the HOMO, and the first reduction step, the LUMO, the energy difference of these two redox processes corresponds to the molecular band gap, which should be recognizable in the optical spectrum.³⁴ This situation has already been discussed extensively for redox processes of metalloporphyrins.³⁵ A value of $2.25 \pm 0.15 \text{ V}$ largely independent of the central metal was found and correlated with the value of 2.18 eV calculated by Gouterman for the HOMO–LUMO difference of a general metalloporphyrin.³⁶ In our case, this potential difference is much smaller. It increases linearly from 1.745 V ($14\,100 \text{ cm}^{-1}$) in $\text{Lu}(\text{OEP})_2$, presumably with the smallest ring–ring distance, to 1.935 V ($15\,500 \text{ cm}^{-1}$) in $\text{La}(\text{OEP})_2$. In the electronic absorption spectrum of 1a–p, a band occurs in the same region ($14\,600$ – $15\,200 \text{ cm}^{-1}$, i.e. 661–684 nm).

Obviously, the redox properties of the double-deckers 1 are determined essentially by the separation of the two tetrapyrrole ligands. We feel that this is due to π – π interactions between the porphyrin ligands, which occur because of the short ring–ring distance. Holten et al.³⁷ have investigated the photophysical properties of $\text{Ce}(\text{OEP})_2$ and found that it was nonfluorescent and

(31) Voegeli, R. H.; Kang, H. C.; Finke, R. G.; Boekelheide, V. *J. Am. Chem. Soc.* **1986**, *108*, 7010–7016.

(32) Allred, A. L. *J. Inorg. Nucl. Chem.* **1961**, *17*, 215–221.

(33) When the redox potential is referred to one electron [eV], the values can be expressed in wavenumbers [cm^{-1}].

(34) Lever, A. B. P.; Licocchia, S.; Magnell, K.; Minor, P. C.; Ramaswamy, B. S. *Adv. Chem. Ser.* **1982**, *No. 201*, 237–252.

(35) (a) Fuhrhop, J.-H.; Kadish, K. M.; Davis, D. G. *J. Am. Chem. Soc.* **1973**, *95*, 5140–5147. (b) Fuhrhop, J.-H. In *Porphyrins and Metalloporphyrins*; Smith, K. M., Ed.; Elsevier: Amsterdam The Netherlands, 1975; pp 593–623.

(36) Gouterman, M. *J. Mol. Spectrosc.* **1961**, *6*, 138–163.

(37) (a) Holten, D., personal communication. (b) Yan, X.; Holten, D. *J. Phys. Chem.* **1988**, *92*, 409–413.

(29) UV/vis [λ_{max} (log ϵ), CH_2Cl_2]: 414 nm (5.42), 484 sh, 550 (3.90), 610 (3.60).

(30) Closs, G. L.; Closs, L. E. *J. Am. Chem. Soc.* **1963**, *85*, 818–819.

that the absorption changes produced by pulse excitation decay largely (>90%) by return of molecules to the ground states in less than 10 ps. These observations were discussed in terms of neutral (π , π^*) exciton states of the two rings, ring-to-ring charge-transfer states and ring-to-metal charge-transfer states. As r_1 of the central ion decreases, the ring-to-ring distance becomes smaller and axial orbital overlap increases. According to our results, the smallest HOMO-LUMO difference and hence the strongest coupling of the two π -electron systems, indeed, is found with Lu(OEP)₂. In the course of the theoretical treatment of the electronic configuration of the special pair, the interaction of two mono(tetra-pyrroles) is likewise taken into account by using a basis set of atomic orbitals for a single "super molecule".⁴

Outlook: Where is the Defect Electron in the π -Radical Double-Deckers? Starting from the intuitive view¹² that the neutral double-deckers containing trivalent metal ions are electron donor-acceptor complexes in which the donor, an (OEP)²⁻ ion, and the acceptor, the (OEP)^{•-} π -radical ion, are held together by a "spacer", the Ln³⁺ ion, the near-IR bands were termed "internal charge-transfer" ("CTI") bands.³⁸ This would imply a hole confined to one ring. However, so far, no evidence has been found in favor of this view. The Eu(OEP)₂ molecule as it exists in the crystal⁶ is isostructural and nearly isodimensional with the closed-shell Ce(OEP)₂ molecule.⁵ Neither the NMR,^{6,9} the ENDOR,⁹ nor resonance Raman spectra¹⁶ give any hint to localization of the hole. Thus, an axially symmetrical electron distribution might be an appropriate description and has been suggested for the bis(π -radical) dimers²⁸ by a simple MO model. Our electrochemical findings would support this view by observing HOMO-LUMO differences that notably decrease on sandwich formation and increase with decreasing ring separation.

When the sandwich radicals are treated as inverse mixed-valence complexes, it is tempting to classify these systems according to Hush's theory.³⁹ This model would imply that compounds of

class II (optical spectra of constituent ions with minor modifications and additional near-IR bands) are encountered in which the energy of the near-IR bands is proportional to the reciprocal distance d of the metals or of the two rings in the inverse case discussed here; i.e., the energy decreases with decreasing distance. However, the energy of the near-IR bands increases with the distance d (see Figure 3). Thus, in this respect, the compounds **1** do not follow Hush's theory. The observed solvent dependence of the energy of the near-IR bands of Eu(OEP)₂⁴⁰ could be interpreted in terms of a ground-state dipole moment becoming smaller in the excited state. This would point to class II compounds with localized holes, but in view of the inconsistency just mentioned, this is only a weak argument.

Nevertheless, the localized hole, hopping with a small thermal activation energy (being about $1/4$ of the CTI level), as suggested by André and co-workers,²¹ is also an attractive alternative to the totally delocalized model. Any final conclusions seem premature at present. The exploitation of the properties of unsymmetrical sandwich systems such as Ce(OEP)(TPP),^{36,41} Eu(OEP)(TPP),⁴¹ Ce(OEP)(Pc),⁴² and Nd₂(Pc)₂(TAP)⁴³ may shed more light on this problem.

Acknowledgment. Financial support of the Deutsche Forschungsgemeinschaft, the Fonds der Chemischen Industrie, the Vereinigung von Freunden der Technischen Hochschule Darmstadt, and the Otto-Röhm-Stiftung is gratefully acknowledged. We thank Dr. B. Speiser for advice and instructions to use his cyclovoltammetry simulation programs and Professor A. Vogler for a helpful discussion. Dr. J.-J. André and Professors D. F. Bocian, D. Holten, K. N. Suslick, and R. Weiss provided their results prior to publication.

(39) Lever, A. B. P. *Inorganic Electronic Spectroscopy*, 2nd ed.; Elsevier: Amsterdam The Netherlands, 1984; pp 647-658.

(40) Near-IR maxima are at 1257 nm (CCl₄), 1250 nm (cyclohexane), or 1215 nm (acetone); measurements are by courtesy of Professor A. Vogler, Regensburg.

(41) Buchler, J. W.; Löffler, J., to be submitted for publication.

(42) De Cian, A.; Fischer, J.; Weiss, R., personal communication.

(43) Moussavi, M.; De Cian, A.; Fischer, J.; Weiss, R. *Inorg. Chem.* **1986**, *25*, 2108-2109.

(38) A reviewer suggested an alternative name for this band: intramolecular charge-transfer ("ICT") band by analogy to the ligand to metal charge-transfer ("LMCT") band in metal complexes. As we have used the name and its abbreviation "CTI" several times already,^{8a,12,14} we prefer to keep it in use.